Carbohydrate Polymers 79 (2010) 145–153

Contents lists available at ScienceDirect

Carbohydrate Polymers

journal homepage: www.elsevier.com/locate/carbpol

Structure and properties of carboxymethyl cellulose/soy protein isolate blend edible films crosslinked by Maillard reactions

Jun-Feng Su [a,b,*], Zhen Huang [a], Xiao-Yan Yuan [b], Xin-Yu Wang [a], Min Li [a]

[a] Institute of Materials Science & Chemical Engineering, Tianjin University of Commerce, Tianjin 300134, China
[b] School of Material Science & Engineering, Tianjin University, Tianjin 300072, China

ARTICLE INFO

Article history:
Received 16 April 2009
Accepted 19 July 2009
Available online 24 July 2009

Keywords:
Carboxymethyl cellulose
Soy protein isolate
Maillard reactions
Blend
Edible films

ABSTRACT

Edible films based on carboxymethyl cellulose (CMC) and soy protein isolate (SPI), compatibilized by glycerol, were prepared by solution casting. The effects of CMC content on blend structure, thermal stability, water solubility and water sorption, and mechanical properties were systematically investigated. Fourier transform infrared (FTIR) spectra showed that Maillard reactions occurred between CMC and SPI, and X-ray diffraction (XRD) scans indicated that the Maillard reactions greatly reduced the crystallinity of SPI. According to differential scanning calorimetry (DSC) analysis, CMC/SPI blends had a single glass transition temperature (T_g) between 75 and 100 °C, indicating that CMC and SPI form one phase blends. Increasing the CMC content improved the mechanical properties and reduced the water sensitivity of blend films. The results indicate that the structure and properties of SPI edible films were modified and improved by blending with CMC.

1. Introduction

Edible films based on agricultural materials have received much attention as potential packaging materials, principally because such biodegradable films are considered to be a promising solution to environmental impacts of synthetic polymer packaging (Wang et al., 2008). Edible films can also be developed with many other functions such as carriers of substances (antimicrobial, aroma, pharmaceutical), coloring agents, or to improve mechanical handling of food (Langmaler, Mokrejs, Kolomamik, & Mladek, 2008). Of the naturally occurring edible materials, soy protein has been widely studied due to its low cost, availability, and complete biodegradability. In particular, soy protein isolate (SPI), with higher protein content than other soy protein products, has superior film-forming ability (Rhim, 2007). It has been reported that SPI edible films have good biodegradability, and high barrier properties against both oxygen and oil at low relative humidity (Cao, Fu, & He, 2007; Mauri and Anon, 2006; Rhim & Lee, 2004). However, there are two inherent problems limiting usage of pure SPI films, namely inadequate mechanical properties and relatively high moisture sensitivity (Rhim, 2004). To improve the mechanical properties and moisture resistance, physical (Kim, Jo, Parke, & Byun, 2008), enzymatic (Chambi & Grosso, 2006), chemical and physicochemical (Shand, Ya, Pietrasik, & Wanasundara, 2007) modifications of SPI have been carried out. It has been confirmed that SPI materials without other secondary components do not show satisfactory physicochemical and mechanical properties for industrial applications (Rhim, 2007). Consequently, addition of other molecules to the protein is essential for modifying the SPI film structure.

Blending is an effective method for modification of polymers because of the strong economic incentives for the use of polymer blends: this method can endow polymers with enhanced properties by conventional processing techniques. It should be emphasized that for edible films, the additives must be safe to eat or generally recognized as safe (GRAS). The additives should be compatible with SPI and have the ability to form films. Carbomethoxy cellulose (CMC), one of the most important derivatives of cellulose, is a typical anionic polysaccharide that has been widely used as a stabilizer in food (Togrul & Arslan, 2004a, 2004b) and can be a suitable additive for enhancing the properties of SPI films. CMC is one of the natural water-soluble cellulose derivatives that have no harmful effects on human health. CMC is used as a highly effective additive to improve product and processing properties in fields of application varying from foodstuffs, cosmetics, and pharmaceuticals to products for the paper and textile industries (Schmitt, Sanchez, Desobry-Banon, & Hardy, 1998). CMC chains are linear β(1→4)-linked glucopyranose residues. In addition, CMC contains a hydrophobic polysaccharide backbone and many hydrophilic carboxyl groups, and hence shows amphiphilic characteristics. Due to its non-toxicity, biocompatibility, biodegradability,

* Corresponding author. Address: Department of Packaging Engineering, Tianjin University of Commerce, Tianjin 300134, China. Tel./fax: +86 22 2621 0595.
E-mail address: sujunfeng2000@yahoo.com.cn (J.-F. Su).

0144-8617/$ - see front matter © 2009 Elsevier Ltd. All rights reserved.
doi:10.1016/j.carbpol.2009.07.035

hydrophilicity, and good film-forming ability, CMC has been used in a number of edible film formulations (Togrul & Arslan, 2004b).

The Maillard reaction can occur when protein is mixed with carbohydrates at elevated temperature (Kim & Lee, 2008). For example, Lii, Chen, Lu, and Tomasik (2003) reported the formation of covalently bonded CMC–casein complex by electrosynthesis. These complexes were very stable to pH and ionic strength changes and exhibited good emulsifying properties and thermal stability.

Based on the considerations outlined above and the motivation of the fundamental research and potential industrial applications of edible films, the objective of the present study work was to fabricate novel edible films based on CMC/SPI blends. Thermal stability, water sorption, water solubility, and mechanical properties were determined for films with varying CMC/SPI weight ratios. In addition, the effects of the Maillard reaction were investigated to understand the relationship between structure and properties.

2. Experimental

2.1. Materials

CMC (food grade, Type FH6©, degree of substitution $x = 0.9$, $M_w = 250{,}000\ g\ mol^{-1}$) was supplied by Hebei Maoyuan Chemical Industry Co., Ltd, China. SPI powder (Type C©) with moisture content <5.0%, prepared by acid precipitation and containing >90% protein, was provided by Harbin High-Technology Soy Protein Co., Ltd, China. Analytical grade glycerol (1,2,3-propanetriol) with 95% purity and sodium hydroxide (NaOH) were acquired from Tianjin Chemical Co., Ltd and used without further treatment. NaOH pellets were used to prepare a $2.0\ mol\ L^{-1}$ solution at room temperature.

2.2. Film fabrication

CMC/SPI blend films were fabricated by solution casting and evaporation. A typical mixed solution of CMC and SPI was prepared by the following steps. (1) Aqueous SPI solution (solution A) was prepared by adding 5 g SPI powder to 100 g of deionized water, whose pH was adjusted to 10.0 with $2.0\ mol\ L^{-1}$ NaOH solution, with continuous stirring at 200 rpm at 80 °C for 60 min. The pH of solution was monitored using an electronic pH-meter (660 Type, Lengpu Co., Shanghai). The reason for using alkaline solution is that pH 10.0 has been found to convert protein molecules to a state of maximum unfolding (Cao et al., 2007). In addition, the high pH induces high lysine–alanine linkage formation, and hydrolysis of asparagines and glutamine primary residues. (2) 10 wt% CMC water solution (solution B) was heated with stirring for 30 min in a water bath maintained at 50 °C. (3) Mixtures of solutions A and B, with and without added glycerol, were thoroughly stirred to form the film fabrication resin. (4) The pH of the blend resin was again adjusted to 10.0 with $2.0\ mol\ L^{-1}$ NaOH solution at 80 °C. (5) The mixed resin, after vacuum defoaming, was poured on a Teflon coated metal sheet to form film. Uniform film thickness was achieved by casting the same amount of film-forming solution on each plate.

The Teflon coated metal sheet was dried in an oven at 50 °C for 6 h then cooled and kept at room temperature for 24 h. Dried films were peeled intact from the casting surface, and maintained at room temperature and 43% relative humidity (produced with saturated K_2CO_3 solution) in a conditioning desiccator for 3 days before use. A series of CMC/SPI/glycerol blends coded as CS-*m*-*n* were prepared by control of the CMC:SPI:glycerol weight ratios, where *m* is weight percent CMC based on the total weight of CMC and SPI, and *n* is the weight percent glycerol based on the total weight of the components of the film.

2.3. Characterization

2.3.1. Fourier transform infrared (FTIR) spectroscopy

FTIR spectra of dried films were obtained using a Nicolet Magna 750 spectrometer with DTGS detector and Omnic 3.2 software. Scanning was carried out in the range 4000–400 cm^{-1} with resolution 4 cm^{-1}, and 128 scans were averaged for each sample.

2.3.2. X-ray diffractometry (XRD)

X-ray diffraction patterns were obtained using a powder diffractometer (Rigaku D/max 2500v/pc, Japan) in the 2θ range 5–50° at $2°\ min^{-1}$ scan rate, with Cu Kα radiation of wavelength 0.1542 nm.

2.3.3. Differential scanning calorimetry (DSC)

DSC analysis was performed using a TA2010 instrument controlled by a TA5000 system (TA Instruments, New Castle, DE, USA). The samples (10 mg) were hermetically sealed in aluminum pans and heated at 5 °C min^{-1} from 0 to 250 °C.

2.3.4. Mechanical properties

Films were conditioned for 2 days in an environmental chamber at 50% relative humidity (RH) and 25 °C before testing. Five samples (25 × 100 mm) of each film were tested. Sample thickness was measured using a micrometer with sensitivity 1 μm. Stress at yield point (σ_y), tensile strength (σ_b), percentage elongation at yield point (P.E.Y.) and percent elongation at break (P.E.B.) were determined with an AG-IS model analyzer (Shimadzu, Japan) according to the ASTM D882-97 (Standard Test Method for Tensile Properties of Thin Plastic Sheeting) procedure at strain rate 5.0 mm min^{-1}. Young's modulus was calculated from the tensile stress–strain plots by the computer software. Duncan's multiple range test ($P < .05$) was used to determine the significance of differences between means.

2.3.5. Thermogravimetric analysis (TGA)

Thermal stability determination was performed with a Dupont SDT-2960 TGA instrument. Sample (50 mg) and reference material (α-Al_2O_3) were heated to 600 °C at 5 °C min^{-1} in flowing (40 mL min^{-1}) nitrogen.

2.3.6. Water solubility

A modification of a reported method (Martelli, Moore, Paes, Gandolfo, & Laurindo, 2006; Martelli, Moore, & Laurindo, 2006) was used to determine the solubility of films in water. Films were cut into pieces (50 × 50 mm) and dried at 60 °C and 96 kPa for 24 h. The weight of each dried film sample, determined to ±0.01 g, was taken as the initial dry weight (W_0) of the sample. Each film sample was immersed in 200 mL of distilled water in a 250-mL beaker. The beakers were capped and heated in a shaking water bath at 25 ± 0.1 °C for a period of time. During the dissolution process, film pieces were removed by use of a pledget, and dried at 60 °C and 96 kPa in a vacuum oven for 24 h to determine the final dry weight (W_1). Percent total soluble matter (S) was calculated from the initial and final dry weights, relative to the initial dry weight, using Eq. (1).

$$S = \frac{W_0 - W_1}{W_0} \times 100\% \quad (1)$$

The solubility of films was determined at 20, 25, 40, 60, 80, and 100 °C using this method.

2.3.7. Water sorption

A modification of a reported method (Taija, Helen, Roos, & Jouppila, 2008) was used to determine the water sorption of films. Film samples, approximately 1.0 g in weight and 10 × 10 mm in size,

were placed in 20 mL glass vials. The glass vials were cooled in a freezer at −20 °C for 5 h (primary drying), then the temperature was reduced to −60 °C at 5 °C min^{-1} (secondary drying). After 24 h, the frozen samples in the glass vials were freeze dried for at least 48 h at a pressure <0.5 mbar. Drying of samples was completed in vacuum desiccators over P_2O_5 for at least 3 days. Water sorption of the film samples was determined at relative humidities 11%, 24%, 33%, 44%, 54%, 66%, 76%, and 86%, in vacuum desiccators over saturated solutions (25 °C) of LiCl, CH_3COOK, $MgCl_2$, K_2CO_3, $Mg(NO_3)_2$, $NaNO_2$, NaCl, and KCl, respectively. Each film sample was supported on a stainless steel lattice on a tripod inside the sorbostats containing the saturated salt solutions, and then the sorbostats were sealed. The sorbostats were then moved into an environmental chamber maintained at a constant temperature. The sample weights were measured at 1 day intervals. Water sorption equilibrium was assumed to have been achieved when the difference between two consecutive sample weights was less than 1.0 mg per g dry solid. Moisture sorption (MS) was calculated at equilibrium for each sample as g water sorbed per 100 g dry film, at each relative humidity. MS data were referred to the dry film weight determined by vacuum drying at 70 °C and pressure <1 mm Hg for 24 h. Triplicate determinations of MS on individually prepared films were carried out for each type of film.

2.3.8. Contact angle determination

Contact angle (θ) of water on film surfaces was measured using a contact angle meter (Digidrop, GBX Co., France) with a ca. 10 μm drop of distilled water on the surface of a film sample with dimensions 3.0 × 3.0 cm.

2.3.9. Surface morphology

Film samples were attached by double sided electrically conductive carbon tape then coated with a thin (~200 Å) layer of gold. The surface morphologies of the film samples were observed by scanning electron microscopy (SEM) using a Philips XL30 instrument at 5 kV accelerating voltage.

3. Results and discussion

3.1. FTIR detection of Maillard reactions

During the preparation of the blending solutions gelation was observed with increasing viscosity. However, the viscosity was

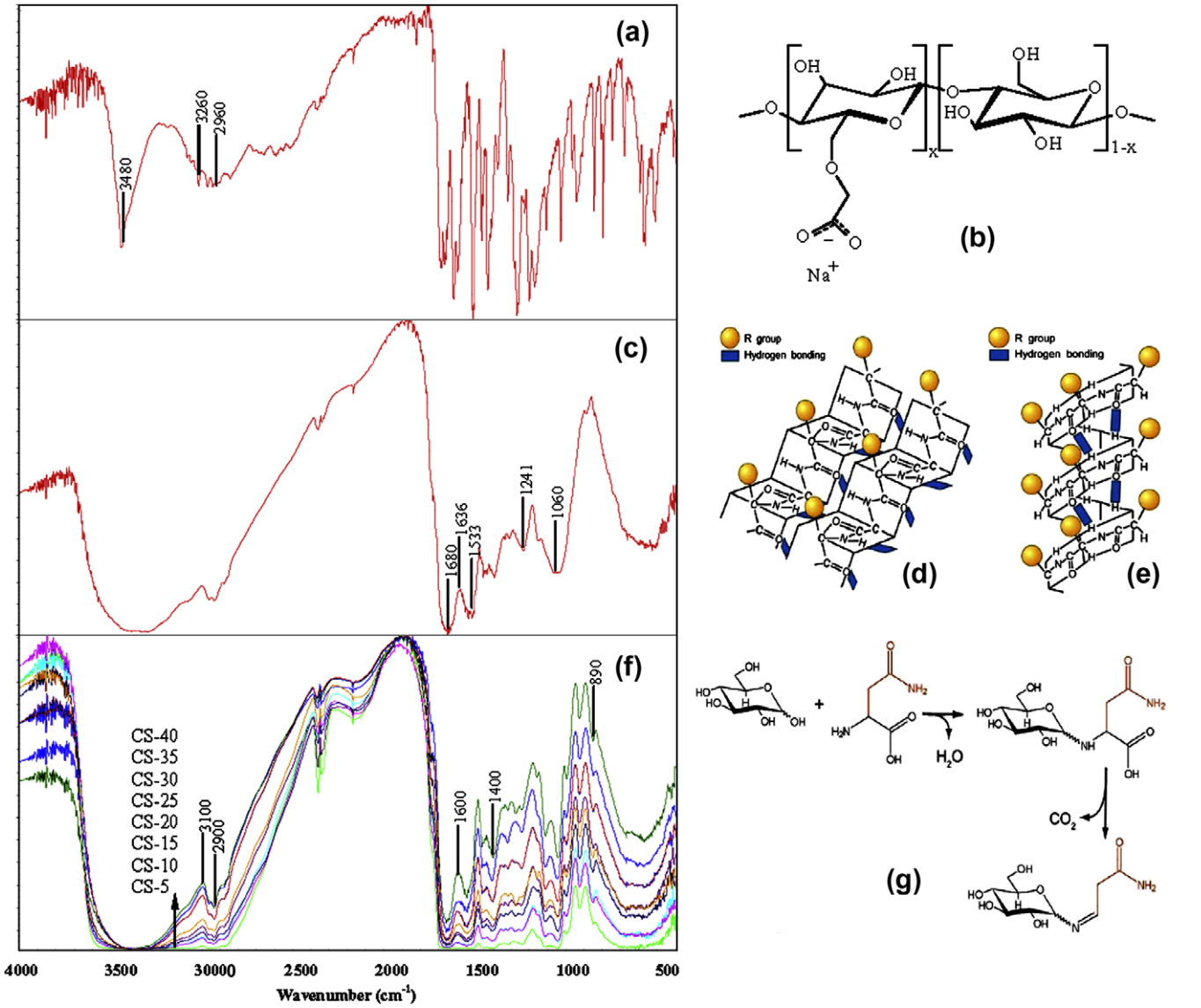

Fig. 1. Maillard reactions tested by FTIR, (a) FTIR spectra of CMC, (b) molecular structure of CMC with degree of substitution *x*, (c) FTIR spectra of SPI, (d and e) α and β molecular structure of SPI, (f) FTIR spectra of CS-5, CS-10, CS-15, CS-20, CS-25, CS-30, CS-35, and CS-40 CMC/SPI blends, (g) a typical Maillard reaction between CMC and an amino acid (glutamine, gln).

not high enough to prevent the fabrication of cast films. The viscosity increase indicated that reaction had occurred between SPI and CMC.

The FTIR analysis was used to identify bands attributable to functional groups present in CMC and SPI. Fig. 1(a) shows the FTIR spectrum of pure CMC powder, and Fig. 1(b) shows the chemical structure of CMC with degree of substitution *x*. The characteristic absorption bands in the ranges 3480–3440, 3260–3270, and 2960–2878 cm^{-1} are assigned to the –OH, –COO, and the –CH stretching regions, respectively. These absorption bands are in accordance with a previous report (Lin, Kumar, Rozman, & Noor, 2005). Fig. 1(c) shows the FTIR spectrum of pure SPI powder. The absorption band at 3294 cm^{-1} arises from hydrogen bonding between protein chains and moisture in the protein. There are obvious –NH bands at 1636–1680 and 1533–1559 cm^{-1}. These bands are in accordance with the reported soy protein spectrum with amide I and amide II bands at 1632 and 1536 cm^{-1}, respectively (Schmidt & Soldi, 2006). The absorption band at 1241–1472 cm^{-1} is attributable to C–N stretching and N–H bending (amide III) vibrations. The band at ca. 1060 cm^{-1} has been attributed to vibrations such as out-of-plane C–H bending (from an aromatic structure) (Rhim, Mohanty, Singh, & Ng, 2006). SPI has a broad molecular weight range (from 8 to about 600 kDa). The various components are identified as 2S, 7S, 11S, and 15S (Svedberg unit), and usually comprise 20–22, 37, 31–40, and 10–11 wt%, respectively, of SPI. Thus, 7S and 11S, (β-conglycinin, 42–58 kDa) and glycinin (360 kDa), respectively, are the two major globulins present in SPI. Fig. 1(d and e) illustrates the α and β structure of SPI macromolecules. SPI possesses many reactive side groups such as $–NH_2$, –OH, and –SH, which can easily participate in crosslinking reactions. These proteins can react with each other to form crosslinks such as disulphide, lysinoalanine, and lanthionine.

Fig. 1(f) shows FTIR spectra of CMC/SPI blend films with various weight ratios. When CMC was added to SPI the intensity of the bands at 3100–2900, 1600–1400, and 890 cm^{-1} gradually decreased. These changes reflect modifications of the amide I band at 1632 cm^{-1}, and the amide II and N–H bending (amide III) vibrations. The absorption band at 1241–1472 cm^{-1} is associated with the C–N stretching vibration. These results show that the –OH group in CMC and amino groups in SPI were consumed during the blending process at elevated temperature. Moreover, a new absorption band appeared at 1647 cm^{-1} indicating a C=N stretching vibration. These phenomena are attributed to Maillard reaction (Aaslyng, Larsen, & Nielsen, 1999; Ajandouz, Desseaux, Tazi, & Puigserver, 2008; Alaiz, Hidalgo, & Zamora, 1999). Fig. 1(g) illustrates a typical Maillard reaction between carboxymethyl cellulose and an amino acid molecule (glutamine, gln). SPI contains 18 kinds of amino acids, connected through peptide bonds to form the primary backbone (Rhim et al., 2006). Consequently, it is easy to envisage that complex Maillard reactions should occur between SPI and CMC. In addition, in the SPI/CMC blends the free amino groups of CMC/SPI films decreased rapidly with increasing CMC addition.

3.2. Assessment of compatibility of blend films by XRD and DSC

XRD was used to investigate crystal structure, and assess the compatibility of SPI and CMC. We confirmed in a previous study that the crystalline structure of SPI was changed through addition of poly(vinyl alcohol) (Su, Huang, Fu, and Liu, 2007). Fig. 2(a–g) shows XRD patterns of (a) pure SPI powder, (b–g) CMC/SPI films CS-5, CS-10, CS-15, CS-20, CS-25, and CS-30. SPI gave a strong characteristic reflection at 2θ about 22°. With increasing CMC content in films, CMC/SPI blends still showed strong reflections at 22°, but the intensity decreased substantially compared with the intensity of the pure SPI reflection. Thus, the crystalline structure of SPI was progressively destroyed by blending with CMC.

Glycerol has always been used in edible films to improve their flexibility. To investigate its effect on compatibility of blend films, XRD curves of samples CS-20-1, CS-20-2, CS-20-3, CS-20-4, and CS-20-5 were obtained and are shown in Fig. 2(h–l). The characteristic reflections of CMC/SPI blend films compatibilized by glycerol had greatly decreased intensities, showing that the presence of glycerol reduced the crystallinity of CMC/SPI blends. This phenomenon occurs through insertion of glycerol into the crystalline structure, thus modifying the microstructure of the blends.

The variation of glass transition temperature (T_g) is another effective indicator of the compatibility of SPI and CMC. Although SPI materials have been widely studied, consistent data relating to T_g for SPI is lacking. A T_g value of about 150 °C obtained by dy-

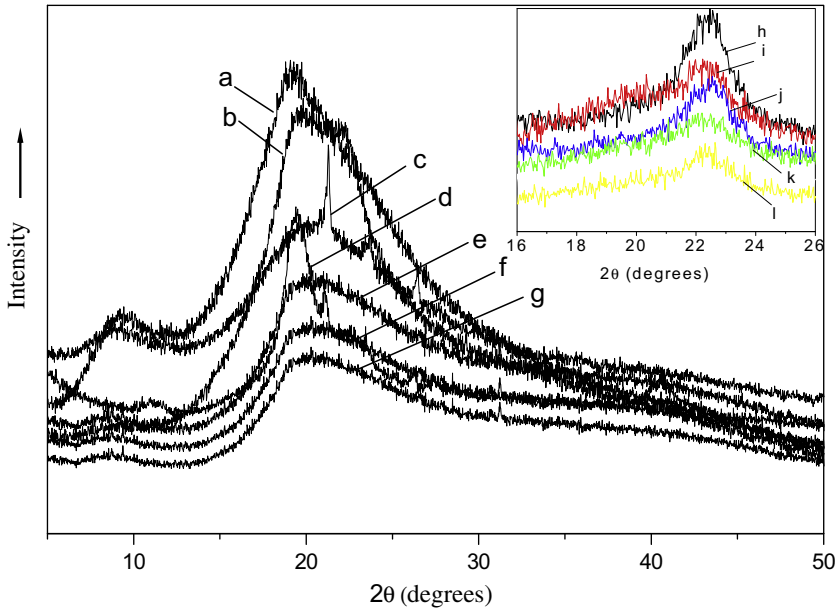

Fig. 2. X-ray patterns of (a) pure SPI powder, (b–g) CS-5, CS-10, CS-15, CS-20, CS-25, and CS-30 CMC/SPI films, (h–l) CS-20-1, CS-20-2, CS-20-3, CS-20-4, and CS-20-5 CMC/SPI/glycerol films.

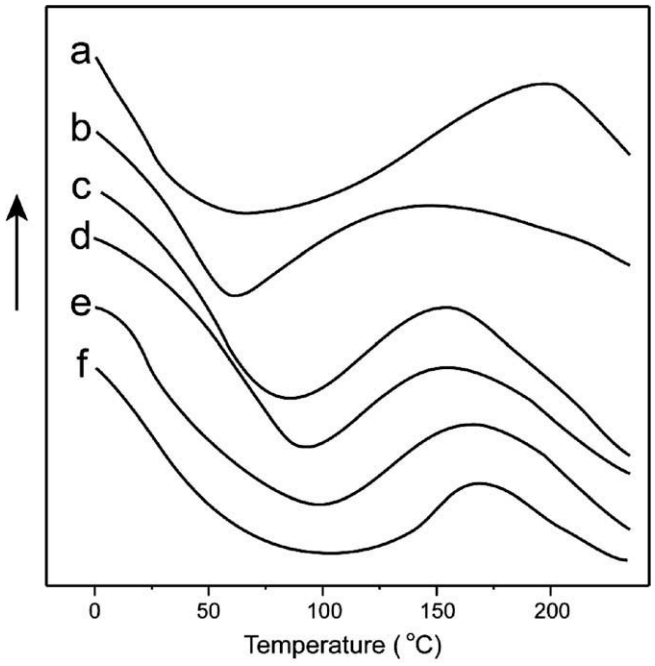

Fig. 3. DSC curves of (a) pure SPI, (b) pure CMC, and (c–f) CMC/SPI blend films of CS-10, CS-20, CS-30, and CS-40.

namic mechanical thermal analysis (DMTA) has been reported for unplasticized SPI, while T_g for SPI plasticized with 25 wt% glycerol decreased to −50 °C (Zhang, Mungara, & Jane, 2001). Wang and co-workers (Wang, Zhang, & Gu, 2005) reported investigation of the glass transition behavior and microstructure of SPI using DSC and XRD. Interestingly, their results revealed two glass transitions for the SPI/glycerol system. All of these investigations imply that the microstructure and glass transition of SPI plasticized by glycerol are still uncertain, due to its structural complexity. Although the magnitude of T_g is still an open question, it needs to be investigated for fabrication and application of SPI films.

DSC curves of pure SPI, pure CMC, CS-10, CS-20, CS-30, and CS-40 blends were analyzed to determine the differences in their thermal behavior. Pure SPI (Fig. 3) had T_g about 60 °C with an endothermic peak, which is similar to our previously reported observations (Su et al., 2007). Two endothermic transition regions have been reported for native SPI (Kumar, Choudhary, Mishra, & Varma, 2004), and attributed to denaturation of β-conglycinin and glycinin fractions of 7S and 11S, respectively. CMC had T_g about 55 °C. CMC/SPI blends showed a single T_g in the range 75–100 °C and melting between 140 and 160 °C. Normally, a single T_g for blended polymers in a DSC scan indicates good compatibility of the component polymers. All blends showed an endothermic peak, at a higher temperature than for SPI and CMC due to the presence of crosslinks in the blends. The endotherm was characterized by the temperature of the endothermic peak. The formation of crosslinks inevitably increases T_g. Consequently, increase in T_g with increasing proportion of CMC is consistent with an increasing extent of crosslinking. The observation of a single glass transition in the DSC heating curves indicates that SPI and CMC are highly compatible.

3.3. Mechanical properties

The mechanical properties of CMC/SPI films varied with the proportion of CMC without considering the degree of substitution in this study. Table 1 lists mechanical property data from stress tests. For CMC/SPI samples without glycerol, the values of σ_y and σ_b increased with increasing CMC content (0–40%) from 41.6 to 53.2 MPa and from 42.0 to 59.2 MPa, respectively. The changes in σ_y and σ_b indicate that molecular entanglement and reaction between SPI and CMC enhanced the tensile strength of the films. A similar result has reported for cellulose derivatives/SPI blends (Zhou, Zheng, Wei, Huang, & Chen, 2008). Although the mechanical properties of the SPI blends depend on the crosslinking methodology, the small glycerol molecule can affect the crystalline structure, glass transition behavior and microstructure of the blends (Chen, & Zhang, 2005).

The small size of the glycerol molecule allows it to penetrate between the polymer chains, and weaken the interaction between SPI and CMC. For each CMC/SPI composition, the values of σ_y and σ_b decreased with addition of glycerol. Moreover, increasing the concentration of glycerol (from 1.0 to 2.0 wt% relative to SPI content) at constant SPI/CMC composition enhanced the reduction of the mechanical properties. More glycerol in a blend leads to less stable and small crystal structures as well as reduced crystallinity (Lodha, & Netravali, 2005). The blends CS-0-1, CS-10-1, CS-20-1, CS-30-1, and CS-40-1 had σ_y values 42.2, 47.0, 50.8, 53.2, and 53.6 MPa, respectively. For CS-0-2, CS-10-2, CS-20-2, CS-30-2, and CS-40-2 the σ_y values were 41.7, 46.9, 50.7, 53.0, and 53.2 MPa. It is clear that increasing the glycerol content for a particular SPI/CMC composition did not significantly decrease the values of σ_y. For each sample, all P.E.Y. and P.E.B. values were increased by addition of

Table 1
Effect of CMC content and compatibilized by glycerol on mechanical properties of CMC/SPI films.

Samples	Thickness (mm)	σ_y (MPa)	σ_b (MPa)	P.E.Y. (%)	P.E.B. (%)	Strength (MPa)	E (MPa)
CS-0-0	0.095 ± 0.006	41.6 d	42.0 e	1.2 f	1.3 j	41.6 d	1227.0 a
CS-10-0	0.094 ± 0.006	46.8 c	46.9 d	2.1 f	20.0 h	31.2 f	1009.2 b
CS-20-0	0.094 ± 0.005	50.6 b	53.6 c	3.4 f	56.1 ef	20.8 g	800.4 d
CS-30-0	0.095 ± 0.003	53.1 a	56.1 d	4.2 e	60.0 e	14.0 h	754.0 d
CS-40-0	0.101 ± 0.002	53.2 a	59.2 a	4.9 d	65.5 e	8.4 i	400.9 g
CS-0-1	0.096 ± 0.006	42.2 d	42.2 e	2.0 f	2.7 j	40.3 d	1227.8 a
CS-10-1	0.095 ± 0.004	47.0 bc	47.5 d	2.5 f	30.8 g	46.8 c	985.0 b
CS-20-1	0.095 ± 0.006	50.8 bc	51.2 cd	4.0 e	66.1 e	55.3 b	600.0 e
CS-30-1	0.095 ± 0.006	53.2 a	53.2 c	4.5 d	110.2 d	58.2 b	621.5 e
CS-40-1	0.103 ± 0.003	53.6 a	53.6 d	5.0 d	125.0 c	61.1 b	200.0 h
CS-0-2	0.095 ± 0.002	41.7 d	42.6 e	2.0 f	15.4 i	40.3 d	1227.4 a
CS-10-2	0.092 ± 0.004	46.9 c	48.5 d	5.0 d	50.4 f	48.2 c	886.3 c
CS-20-2	0.093 ± 0.004	50.7bc	54.1 c	7.1 c	125.7 c	57.3 b	580.0 e
CS-30-2	0.105 ± 0.005	53.0 a	55.2 bc	15.0 b	139.2 b	59.0 b	520.2 f
CS-40-2	0.109 ± 0.003	53.2 a	57.4 a	25.1 a	159.0	65.4 a	187.4 h

σ_y is the stress at yield point, σ_b is the stress at break point, P.E.Y. is the percentage elongation at yield point, P.E.B. is the percentage elongation at break point, E is Young's modulus; CMC/SPI-0-0 means SPI/PVA (100/0) without glycerol, CS-10-2 means CMC/SPI (100/10) compatibilized by glycerol (2 wt% SPI). Means values were determined in five replicates. Alphabets in a column indicate significant difference at $P < .05$ by Duncan's multiple range tests.

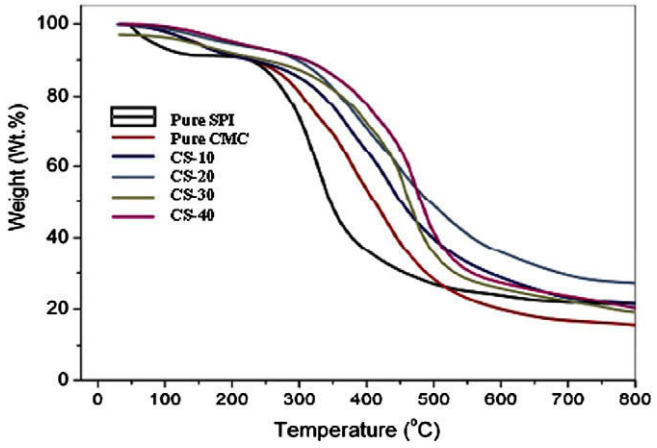

Fig. 4. TGA curves of pure SPI, pure CMC, CS-10, CS-20, CS-30, and CS-40 blend films.

glycerol to the blends. For example, the values of P.E.Y. for CS-10, CS-10-1, and CS-10-2 were 2.1%, 2.5%, and 5.0%, and the P.E.B. values for CS-10, CS-10-1, and CS-10-2 were 20.0%, 30.8%, and 50.4%. The values of Young's modulus decreased with addition of glycerol, which indicates that the blend becomes softer due to plasticization by glycerol. Soy protein contains polar and non-polar side chains and there are hydrogen bonding, dipole–dipole, charge–charge, and hydrophobic intermolecular interactions. The strong charge and polar interactions between side chains of soy protein molecules restrict segment rotation and molecular mobility, which lead to increases in modulus, stiffness, yield point and tensile strength (Zhang, Mungara, & Jane, 2001). As a plasticizer, glycerol reduces the interaction between protein molecules and increases the flexibility, extensibility, and processability of SPI polymers (Su et al., 2007).

The enhanced mechanical properties of SPI/CMC blends (compared to SPI) can be attributed to the long-chain CMC molecules, which contain many –OH groups that participate in strong intermolecular interactions with protein molecules. These interactions may include hydrogen bonding, dipole–dipole, and charge effects. In addition, blending the long CMC molecules with SPI increases molecular entanglements, which in turn improve the mechanical properties of SPI. Moreover, the new bonds between protein and cellulose formed by the Maillard reaction also contribute to improvement of mechanical properties (Ajandouz et al., 2008; Yasir, Sutton, Newberry, Andrews, & Gerrard, 2007). Nagahama confirmed that the crosslinking effect of Maillard reaction improved the tensile strength of chitin/gelatin membranes (Nagahama et al., 2008).

3.4. Thermal stability assessment by TGA

Fig. 4 shows TGA scans of pure SPI, pure CMC and CMC/SPI films (CS-10, CS-20, CS-30, and CS-40). SPI has a relatively low decomposition temperature (about 110 °C) according to our previous study

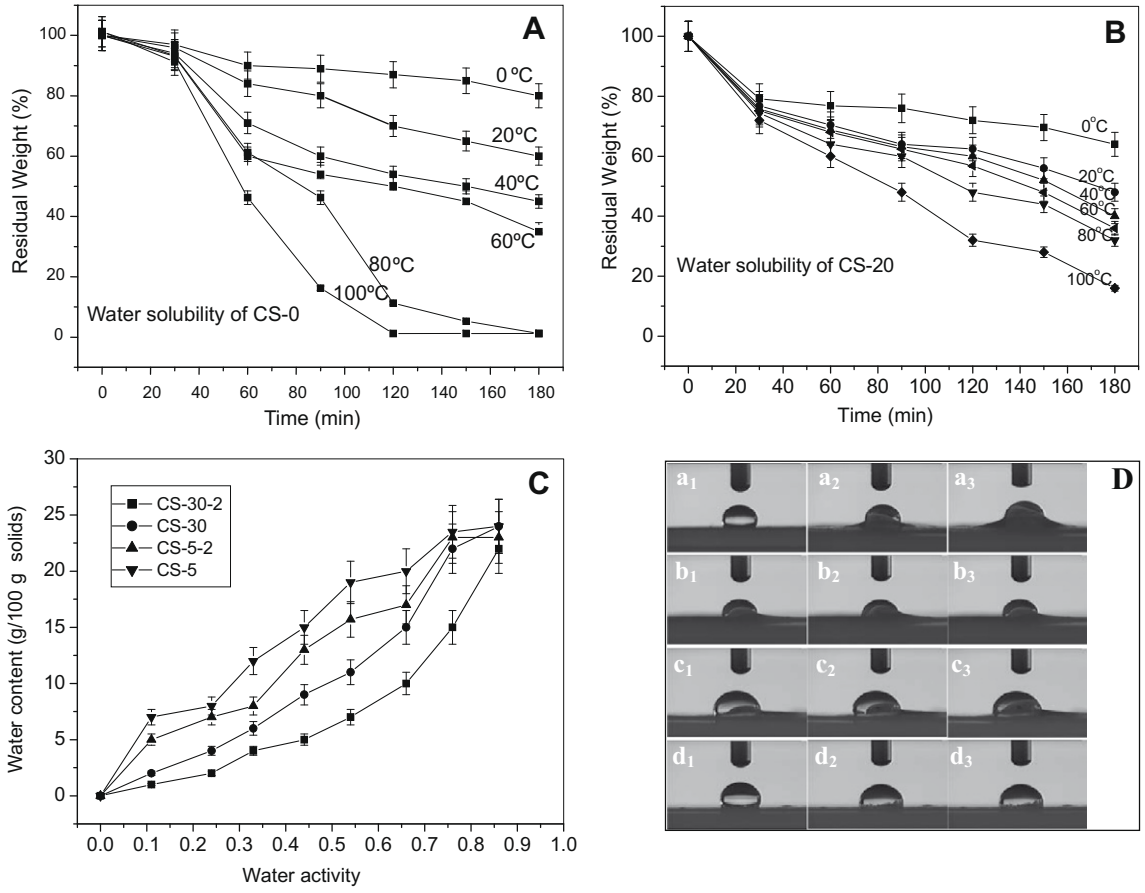

Fig. 5. Water solubility and water sorption of films: water solubility of (A) CS-0 and (B) CS-10 in water with different temperatures; (C) water sorption of CS-5, CS-5-2, CS-30, and CS-30-2 films, (D) contact angle tests of the wetting process of CS-20 (a_1, a_2), CS-20-1 (b_1, b_2), CS-20-2 (c_1, c_2), and CS-20-3 (d_1, d_2), two photos were taken for each sample at the 5 and 10 s time after water dropped on the surface of films.

(Su et al., 2007). There is an initial weight loss of about 10% for SPI that is due to loss of moisture below 100 °C. CMC starts to decompose at about 180–210 °C and its weight loss sharply in the temperature range 300–500 °C. The observed CMC decomposition behavior is similar to reported results (Uskokovic, 2008). Commonly, CMC decomposes in a two-stage process. The initial weight loss is attributed to the presence of a small amount of moisture, and the second weight loss arises from CO_2 from the COO^- groups of CMC (Ma, Chang, & Yu, 2008).

The TGA scans for CMC/SPI blends showed about 15% weight loss due to moisture in the temperature range 0–150 °C. However, these samples have different decomposition ratios in the 80–30% residual mass range. CS-10 had the largest slope of the weight versus temperature plot in this region. With increasing CMC content of the CMC/SPI blends, the slope of the weight–temperature line is reduced, implying that the blend films had greater thermal stability than pure SPI. In addition, the TGA curves of all of the blends showed a decomposition temperature in the range 250–350 °C, which was higher than the decomposition temperatures of both SPI and CMC. All film samples exhibited a single decomposition temperature in their TGA curves, which may also indicate that CMC and SPI have good compatibility. The enhanced thermal stability of the blends can be attributed to crosslinking and Maillard reaction between CMC and SPI.

3.5. Water solubility and water sorption

Measuring solubility in water is another method to assess the thermal stability of soluble films (Yin, Tang, Wen, & Yang, 2007). CMC is water soluble and SPI is water sensitive, which results in the water sensitivity of their blends. As a 'green' polymeric material, CMC/SPI needs to have relatively good stability in water for an extended service time in applications. Consequently, decreased water sensitivity for the blend films is very meaningful for the applications of these films. The water solubility is usually determined by the molecular structure, including crystallinity and crosslinking. Structure and thermal stability information may be obtained through solubility tests (Tsukada et al., 2006).

The water solubility of samples of CS-0 and CS-20 blend films was measured. The solubility of these films in water at various temperatures is shown in Fig. 5(A and B). Comparison of the residual masses of CS-0 and CS-20 led to the following observations. (1) The rate of dissolution increased with increasing water temperature, for both samples; (2) CS-10 dissolved more slowly than CS-0; (3) CS-0 was completely dissolved in 180 min in water at 100 °C, whereas for CS-10 there was about 20% residual (undissolved) mass under those conditions. The implication is that crosslinking reactions occurred between CMC and SPI during formation of the blend films, confirming that the Maillard reaction occurred. The crosslinks can prolong the resistance of film to hot water (Tahaei, Abdouss, Edrissi, Shoushtari, & Zargaran, 2008). The comparison of dissolution rates shows that blending of CMC with SPI significantly enhances the thermal stability of pure SPI film.

Proper modeling and optimization of the film drying process requires knowledge of sorption isotherms at different temperatures. Moreover, water sorption isotherms reflect significant details of film microstructure. Generally, the amount of water absorbed by the films increased with increasing water activity. Fig. 5(C) shows water sorption data for CMC/SPI films of the blends CS-5, CS-5-2, CS-30, and CS-30-2. With the increasing CMC content, the water sorption ability of films decreased, and addition of glycerol (e.g., to CS-5 film) decreased water sorption. However, the water contents of plasticized and unplasticized films were nearly equal at 88% RH (water activity = 0.88). Moreover, water content corresponding to a water monolayer for films without plasticizer and with 22% plasticizer content was attained at that water activity.

Water contact angle (θ) of film is another indicator for direct determination of the hydrophilicity of films. The final state of the water drop on the film surface is taken as an indication of the wettability of the surface by water. To understand the effect of plasticizer on film wettability, we investigated the contact angles of sample CS-20 with various glycerol contents. In contrast with synthetic polymer films, the contact angles of the natural material films decreased rapidly with contact time. Two photographs were taken for each sample 5 and 10 s after water was dropped on the surfaces of the films. Fig. 5(D) shows the wetting process of samples of CS-20 (a_1, a_2), CS-20-1 (b_1, b_2), CS-20-2 (c_1, c_2), and CS-20-3 (d_1, d_2). CS-20 had a relatively high contact angle, and plasticization with glycerol decreased the contact angle. Swelling of the

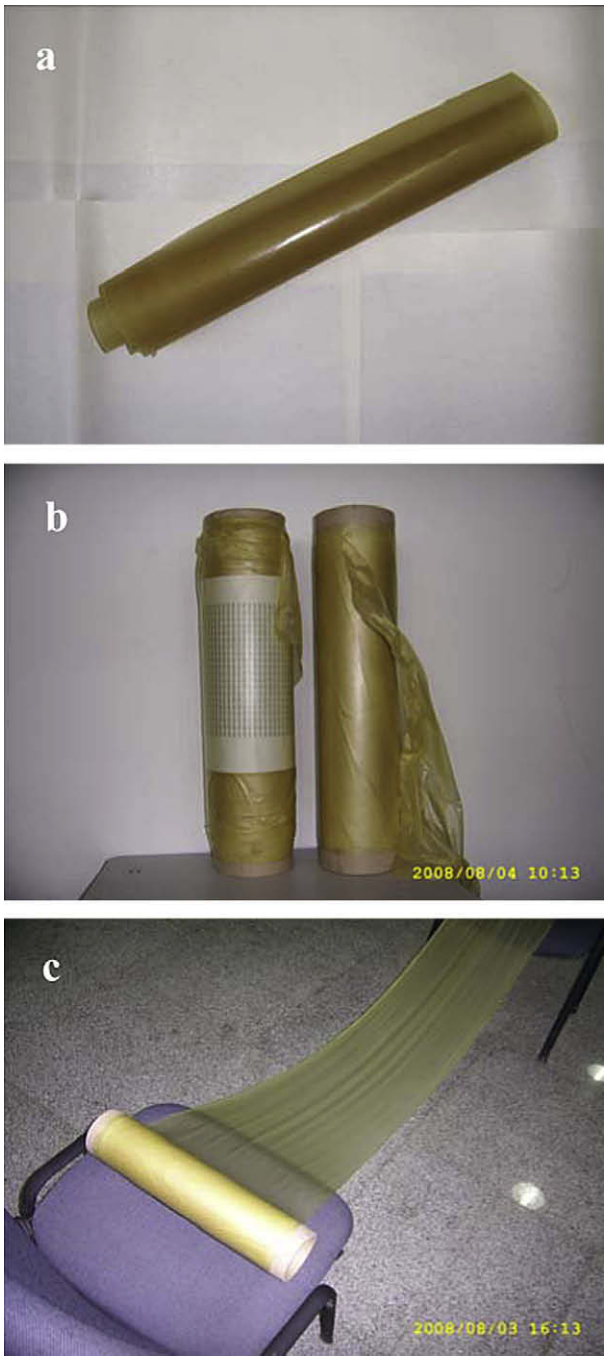

Fig. 6. Photographs of CMC/SPI films in expanding and rolling states fabricated by a continuous casting method.

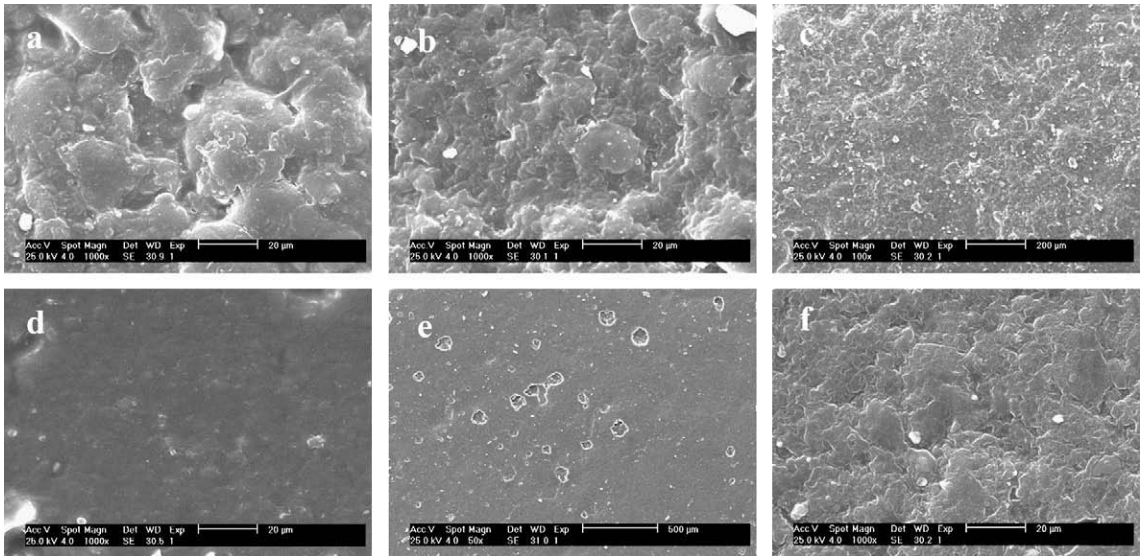

Fig. 7. SEM surface morphologies of (a–d) CS-10 and CS-20 samples with/without 1.0 wt% glycerol; (e and g) CS-10 and CS-10-1 after water vapor transmission tests.

water drop also provides information. For the films made from CS-20-2 and CS-20-3 with increased plasticizer, water absorption by the films was apparent from swelling of the polymer with the water drop. Though glycerol can improve the flexibility of CMC/SPI films, it also enhances the moisture sensitivity of the films.

3.6. Surface morphology of blend films

Fig. 6(a–c) shows photographs of CMC/SPI films in expanded and rolled states fabricated by a continuous casting method. It is apparent that these films can be fabricated smoothly without cracks and micro-holes. All of the films had good toughness, and were sufficiently soft enough to be rolled into forms for practical applications.

Fig. 7(a–d) shows SEM surface morphologies of CS-10 and CS-20 samples with and without 1.0 wt% glycerol to understand the effect of glycerol addition on the microstructure of CMC/SPI films. Both films appeared to have a dense structure at lower magnification. However, some porosity was detected, although these cavities seem to be closed pores. Such closed porous were previously observed in pure SPI films (Su et al., 2007), indicating that blending with CMC cannot completely eliminate the structural defects of SPI. Compared to CS-10 and CS-20, CS-10-1, and CS-20-1 have more compact surface structures, showing that a continuous matrix is not formed in the pure CMC/SPI films because there is no plasticizer for increasing association with the long-chain polymers. In addition, the differences observed in film structures can be due mainly to interactions promoted by the temperature and humidity conditions employed. After the water vapor transmission determination (see Fig. 7(e and g)), the pores in sample CS-10 had been enlarged to micro-holes by the action of water molecules. However, CS-10-1 still had a continuous matrix without porous and holes. The larger number of hydrophilic interactions in the CMC/SPI/glycerol film enhances water diffusion through the film, and confers inferior barrier properties to water vapor and higher water solubility than is the case for unplasticized CMC/SPI films.

4. Conclusions

Food grade CMC and SPI were successfully employed to fabricate novel edible cast films. The compatibility of the component polymers, and mechanical properties, thermal stability, water solubility and water sorption of SPI/CMC blend films were investigated. CMC/SPI films have higher tensile strength (σ_b) and percent elongation at break point (P.E.B.) than do pure SPI films. Plasticization with glycerol reduces Young's modulus of the blend films. XRD reveals that CMC and SPI are highly compatible, and addition of glycerol reduces the crystallinity of CMC/SPI blends. The observation of a single glass transition by DSC confirms the conclusion from XRD that CMC and SPI form homogeneous, single phase blends. The water sensitivity of films decreases with increasing CMC content, and the improvement in properties achieved by blending CMC with SPI is attributed to Maillard reaction occurring between CMC and SPI. The films developed in this work are suggested to be suitable for low moisture foods and pharmaceutical products.

Acknowledgements

The authors gratefully acknowledge the support of National Key Technology R&D Program of China (2006BAD05A05), the Students Research Training of Tianjin University of Commerce (SRT, 2008038) and the help of Harbin High-Tech Soybean Food Co., Ltd.

References

Aaslyng, M. D., Larsen, L. M., & Nielsen, P. M. (1999). The influence of maturation on flavor and chemical composition of hydrolyzed soy protein produced by acidic and enzymatic hydrolysis. *Zeitschrift Fur Lebensmittel-Untersuchung Und-Forschung a-Food Research and Technology, 208*(5–6), 355–361.

Ajandouz, E. H., Desseaux, V., Tazi, S., & Puigserver, A. (2008). Effects of temperature and pH on the kinetics of caramelisation, protein cross-linking and Maillard reactions in aqueous model systems. *Food Chemistry, 107*(3), 1244–1252.

Alaiz, M., Hidalgo, F. J., & Zamora, R. (1999). Effect of pH and temperature on comparative antioxidant activity of nonenzymatically browned proteins produced by reaction with oxidized lipids and carbohydrates. *Journal of Agricultural and Food Chemistry, 47*(2), 748–752.

Cao, N., Fu, Y. H., & He, J. H. (2007). Preparation and physical properties of soy protein isolate and gelatin composite films. *Food Hydrocolloids, 21*(7), 1153–1162.

Chambi, H., & Grosso, C. (2006). Edible films produced with gelatin and casein cross-linked with transglutaminase. *Food Research International, 39*(4), 458–466.

Chen, P., & Zhang, L. (2005). New evidences of glass transitions and microstructures of soy protein plasticized with glycerol. *Macromolecular Bioscience, 5*(3), 237–245.

Kim, J. K., Jo, C., Parke, H. J., & Byun, M. W. (2008). Effect of gamma irradiation on the physicochemical properties of a starch-based film. *Food Hydrocolloids, 22*(2), 248–254.

Kim, J. S., & Lee, Y. S. (2008). Effect of reaction pH on enolization and racemization reactions of glucose and fructose on heating with amino acid enantiomers and

formation of melanoidins as result of the Maillard reaction. *Food Chemistry, 108*(2), 582–592.
Kumar, R., Choudhary, V., Mishra, S., & Varma, I. K. (2004). Enzymatically modified soy protein. Part I. Thermal behavior. *Journal of Thermal Analysis and Calorimetry, 75*, 727–738.
Langmaler, F., Mokrejs, P., Kolomamik, K., & Mladek, M. (2008). Biodegradable packing materials from hydrolysates of collagen waste proteins. *Waste Management, 28*(3), 549–556.
Lii, C. Y., Chen, H. H., Lu, S., & Tomasik, P. (2003). Electrosynthesis of kappa-carrageenan complexes with gelatin. *Journal of Polymers and the Environment, 11*(3), 115–121.
Lin, O. H., Kumar, R. N., Rozman, H. D., & Noor, M. A. M. (2005). Grafting of sodium carboxymethylcellulose (CMC) with glycidyl methacrylate and development of UV curable coatings from CMC-g-GMA induced by cationic photoinitiators. *Carbohydrate Polymers, 59*(1), 57–69.
Lodha, P., & Netravali, A. N. (2005). Thermal and mechanical properties of environment-friendly 'green' plastics from stearic acid modified-soy protein isolate. *Industrial Crops and Products, 21*(1), 49–64.
Ma, X. F., Chang, P. R., & Yu, J. G. (2008). Properties of biodegradable thermoplastic pea starch/carboxymethyl cellulose and pea starch/microcrystalline cellulose composites. *Carbohydrate Polymers, 72*(3), 369–375.
Martelli, S. M., Moore, G. R. P., & Laurindo, J. B. (2006). Mechanical properties, water vapor permeability and water affinity of feather keratin films plasticized with sorbitol. *Journal of Polymers and the Environment, 14*(3), 215–222.
Martelli, S. M., Moore, G., Paes, S. S., Gandolfo, C., & Laurindo, J. B. (2006). Influence of plasticizers on the water sorption isotherms and water vapor permeability of chicken feather keratin films. *Lwt-Food Science and Technology, 39*(3), 292–301.
Mauri, A. N., & Anon, M. C. (2006). Effect of solution pH on solubility and some structural properties of soybean protein isolate films. *Journal of the Science of Food and Agriculture, 86*(7), 1064–1072.
Nagahama, H., Kashiki, T., Nwe, N., Jayakumar, R., Furuike, T., & Tamura, H. (2008). Preparation of biodegradable chitin/gelatin membranes with GlcNAc for tissue engineering applications. *Carbohydrate Polymers, 73*(3), 456–463.
Rhim, J. W. (2004). Increase in water vapor barrier property of biopolymer-based edible films and coatings by compositing with lipid materials. *Food Science and Biotechnology, 13*(4), 528–535.
Rhim, J. W. (2007). Mechanical and water barrier properties of biopolyester films prepared by thermo-compression. *Food Science and Biotechnology, 16*(1), 62–66.
Rhim, J. W., & Lee, J. H. (2004). Effect of $CaCl_2$ treatment on mechanical and moisture barrier properties of sodium alginate and soy protein-based films. *Food Science and Biotechnology, 13*(6), 728–732.
Rhim, J. W., Mohanty, K. A., Singh, S. P., & Ng, P. K. W. (2006). Preparation and properties of biodegradable multilayer films based on soy protein isolate and poly(lactide). *Industrial & Engineering Chemistry Research, 45*(9), 3059–3066.
Schmidt, V., & Soldi, V. (2006). Influence of polycaprolactone-triol addition on thermal stability of soy protein isolate based films. *Polymer Degradation and Stability, 91*(12), 3124–3130.
Schmitt, C., Sanchez, C., Desobry-Banon, S., & Hardy, J. (1998). Structure and technofunctional properties of protein–polysaccharide complexes: A review. *Critical Reviews in Food Science and Nutrition, 38*(8), 689–753.
Shand, P. J., Ya, H., Pietrasik, Z., & Wanasundara, P. (2007). Physicochemical and textural properties of heat-induced pea protein isolate gels. *Food Chemistry, 102*(4), 1119–1130.
Su, J. F., Huang, Z., Liu, K., Fu, L. L., & Liu, H. R. (2007). Mechanical properties, biodegradation and water vapor permeability of blend films of soy protein isolate and poly (vinyl alcohol) compatibilized by glycerol. *Polymer Bulletin, 58*(5–6), 913–921.
Tahaei, P., Abdouss, M., Edrissi, M., Shoushtari, A. M., & Zargaran, M. (2008). Preparation of chelating fibrous polymer by different diamines and study on their physical and chemical properties. *Materialwissenschaft und Werkstofftechnik, 39*(11), 839–844.
Taija, R. A., Helen, H., Roos, Y. H., & Jouppila, K. (2008). Effect of type and content of binary polyol mixtures on physical and mechanical properties of starch-based edible films. *Carbohydrate Polymers, 71*(2), 269–276.
Togrul, H., & Arslan, N. (2004a). Carboxymethyl cellulose from sugar beet pulp cellulose as a hydrophilic polymer in coating of mandarin. *Journal of Food Engineering, 62*(3), 271–279.
Togrul, H., & Arslan, N. (2004b). Extending shelf-life of peach and pear by using CMC from sugar beet pulp cellulose as a hydrophilic polymer in emulsions. *Food Hydrocolloids, 18*(2), 215–226.
Tsukada, H., Takano, K., Hattori, M., Yoshida, T., Kanuma, S., & Takahashi, K. (2006). Effect of sorbed water on the thermal stability of soybean protein. *Bioscience Biotechnology and Biochemistry, 70*(9), 2096–2103.
Uskokovic, V. (2008). Composites comprising cholesterol and carboxymethyl cellulose. *Colloids and Surfaces B – Biointerfaces, 61*(2), 250–261.
Wang, L. Z., Liu, L., Holmes, J., Huang, J., Kerry, J. F., & Kerry, J. P. (2008). Effect of pH and addition of corn oil on the properties of whey protein isolate-based films using response surface methodology. *International Journal of Food Science and Technology, 43*(5), 787–796.
Wang, N. G., Zhang, L. N., & Gu, J. M. (2005). Mechanical properties and biodegradability of crosslinked soy protein isolate/waterborne polyurethane composites. *Journal of Applied Polymer Science, 95*(2), 465–473.
Yasir, S. B. M., Sutton, K. H., Newberry, M. P., Andrews, N. R., & Gerrard, J. A. (2007). The impact of Maillard cross-linking on soy proteins and tofu texture. *Food Chemistry, 104*(4), 1502–1508.
Yin, S. W., Tang, C. H., Wen, Q. B., & Yang, X. Q. (2007). Properties of cast films from hemp (*Cannabis sativa* L.) and soy protein isolates. A comparative study. *Journal of Agricultural and Food Chemistry, 55*(18), 7399–7404.
Zhang, J., Mungara, P., & Jane, J. (2001). Mechanical and thermal properties of extruded soy protein sheets. *Polymer, 42*(6), 2569–2578.
Zhou, Z., Zheng, H., Wei, M., Huang, J., & Chen, Y. (2008). Structure and mechanical properties of cellulose derivatives/soy protein isolate blends. *Journal of Applied Polymer Science, 107*(5), 3267–3274.